ANNALS OF GEOPHYSICS, 63, 5, PA553, doi:10.4401/ag-7933

Energetic Particle Flux Variations around magnetic storm and huge earthquake

Jianping Huang*,[1,2], Xuhui Shen[1], Wenjing Li[1], Wei Chu[1]

(1) National Institute of Natural Hazards, Ministry of Emergency Management, Beijing 100085, China
(2) Institute of Disaster Prevention, Sanhe 065201, China

Article history: received September 19, 2018; accepted February 3, 2020

Abstract

A megathrust earthquake with Mw 9.0 occurred in the North-western Pacific Ocean on March 11, 2011. From the energetic particle flux from WIND, CLUSTER and GOES in different L locations, some variation can be found around the earthquake. Among the three satellites, WIND is used to identify solar activity, and GOES is used to detect the changes from ground source. And during the same period, a magnetic storm with intensity -80nT occur. In order to validate the particle flux variation, multi-parameters relationship is compared. The results show that: (1) all energetic fluxes variation can reflect the solar activity. The far ones are connected with the F10.7 and the near ones are connected with Dst/Kp. (2) The energetic particle fluxes give a scarp change in all energy bands at the beginning coupling period and when the space recovers to be quite, the fluxes will have a long decreasing tail from high to low energy. (3) The coseismic and after effect have been detected in GOES and the pre-seismic emission should exist because the bigger decreasing fluxes in GOES are responding to the period with smaller Kp.

Keywords: Energetic particle, different altitudes, earthquake.

1. Introduction

At 05:46 (UTC) On March 11, 2011, an M9.0 earthquake occurred near Miyagi city (142.6° E, 38.1° N), off the east coast of Honshu, Tohoku area, Japan. The resultant tsunami waves damaged countless coastal communities around the Tohoku area. This earthquake is the strongest event taken place in the last 20 years. From the Japanese GPS network, the Total Electron Content (TEC) in the ionosphere above the focal region rapidly increases 40 minutes before the event [Heki, 2011, 2013; Jin, 2014]. The earthquake and the tsunami, coupling with the atmosphere, generated upward-propagating atmospheric disturbances, which reached the upper atmosphere and ionosphere, and were subsequently detected by GPS receivers [Galvan et al., 2012; Komjathy et al., 2012; Yu et al., 2015]. Those pre-seismic signals have been validated by the Lithosphere-Atmosphere-Ionosphere Coupling (LAIC) theory [Pulinets et al., 2000, 2004 and 2011; Zhao et al., 2010; Kuo et al., 2014; Zhang, et al., 2012].

According to the LAIC, the ionospheric disturbance is originated from electromagnetic field or associated with waves above strong earthquake regions [Parrot, 2012]. In addition to the TEC or electron density, the electromagnetic field and energetic particle flux can also be disturbed. It is worth noting that, the physics of the solar-terrestrial environment is governed principally by the interaction of energetic charged particles with electric and magnetic fields in space. In particular, near the Earth, most of these charged particles derive their energy ultimately from the Sun, directly or through the interaction of the solar wind with the Earth's magnetosphere [Russell, et al, 2016]. Wave-particle interactions also play a fundamental role in energy exchange between plasma waves and radiation belt electrons [Walt, 1994]. Meanwhile, the similar process, but in the opposite direction, has been suggested. Before strong earthquakes, some EM waves, especially the VLF/ELF wave, can be emitted from the lithosphere [Merzer et al., 1997; Molchanov et al., 1998; Zhang X et al., 2014], penetrates into the ionosphere through atmosphere [Rozhnoi et al., 2008 and references therein], and couples with the ionospheric plasma and energetic particles [Nemec, et al., 2009].

Energetic particle variation, called precipitation or enhancement, has been taken as the pre-seismic precursor since 1980s [Galper et al., 1989]. After more and more attentions were paid on the relation between particles and earthquakes in terms of a number of parameters, including time difference, spatial shift according to case study, statistical analysis or some modeling based on wave-particle coupling theory [Voronov et al., 1990; Galper et al., 1992, 1995; Pustovetov et al., 1993; Aleksandrin et al., 2003; Sgrigna et al., 2005; Huang et al., 2010; Li et al., 2012; Fidani, 2010; Zhang et al., 2013; Wang et al., 2014].

All these studies showed that before strong earthquakes, energetic particle flux would be affected from 300 to 2000 km altitudes [Wang et al., 2014; Zhang et al., 2013]. However, when a magnetic storm and a strong earthquake happened at the same time, what does the energetic particle response? In this paper, we are devoted to exam whether the pre-seismic flux variation could be found at higher altitudes. So, the higher altitudes data from WIND, Cluster II and GOES are collected, and the time period are set around the occurrence of the M9.0 Tohoku earthquake.

2. Space weather background and satellite observation

2.1 Space weather background

Several space weather indexes are shown in Figure 1, including f 0.7, Kp, Dst, AU, AL and solar Lyman-alpha.

F10.7, the solar radio flux at 10.7 cm (2800 MHz) is an excellent indicator of solar activity. From March1 to March 15, the level increased and reached maximum on March 8 and then decreased.

Kp, the geomagnetic three-hourly index, is considered a proxy for the energy input from the solar wind to Earth. During the period, the high value occurred on March 10-12.

Dst index represents the axially symmetric disturbance magnetic field at the dipole equator on the Earth's surface. Major disturbances in Dst are negative, namely decreases in the geomagnetic field. These field decreases are produced mainly by the equatorial current system in the magnetosphere, usually referred to as the ring current. Only on March 11, the Dst decreased lower than -80nT.

The trend of the AU and AL is similar to Dst. And the solar Lymann-alpha is almost same to F10.7.

2.2 Satellite data source

Many satellites have been launched into various locations to study the small-scale plasma structures in three dimensions in key plasma regions, such as the solar wind, bow shock, magnetopause, polar cusps, magnetotail and the auroral zones. Here WIND, CLUSTER, and GOES are introduced, which are located in about 200 Re, 1.2~19 Re, 5~6 Re (Earth radii, where 1 RE = 6371 km).

2.3 Wind observatory

Figure 2 lists the magnetism and energetic particle records (Three-Dimensional Plasma and Energetic Particle Investigation payload, 3DP) from WIND satellite.

The variation shape is similar in the three components of the magnetic field. And the amplitude of Bx is larger than that of By and Bz. The disturbance occurred on March 10 to 12. The clear sharp changes on March 10 and March 11.

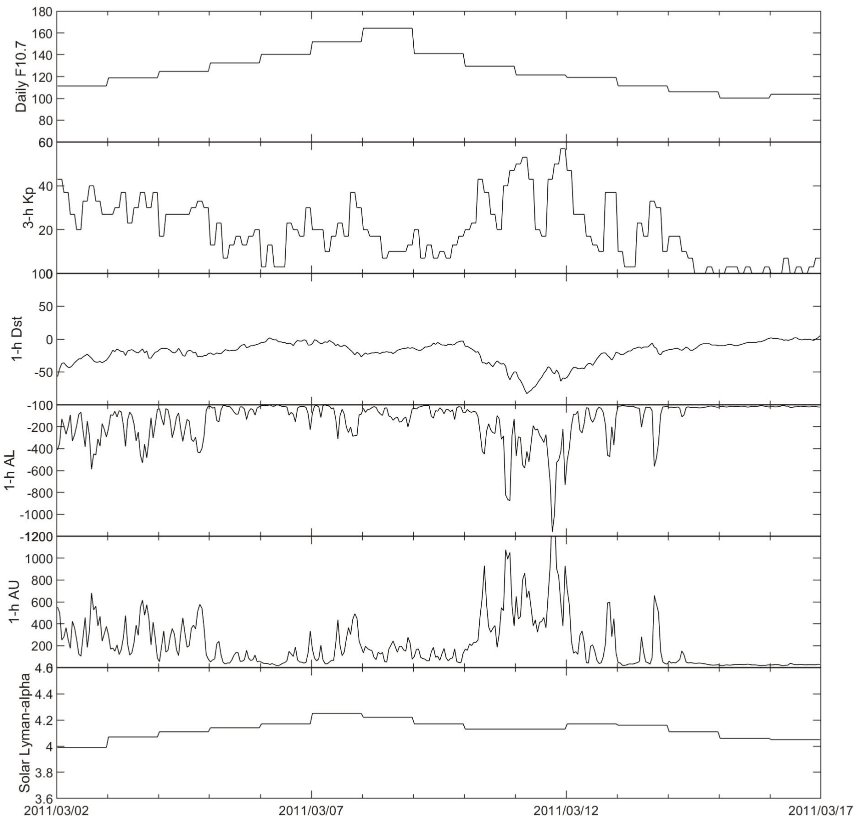

Figure 1. Space weather index from February 20 to March 20, 2011.

For all the energetic fluxes, three "layers" can be found: the undisturbed region (blue region), the weak increased region (green region) and the core enhancement region (red region). All 4 payloads recorded the changes. The shape at the increased layer is sudden scarp and then weak slope, as shown in SOSP, SFSP and EHSP. The shape in the core enhancement region is like "Gauss shape". The center data of Gauss shape is March 10 for all payloads and also is March 11 in EHSP and ELSP. An indentation, as shown in SOSP, ELSP and not clear in SFSP and EHSP, can also be found in Figure 2. The difference is the starting-ending date and energy range, as listed in Table 1.

Table 1 listed the variation date and energy for all payloads. For ELSP, no obvious changes can be seen in the increased layer. The date in SFSP and EHSP is several hours earlier than that in SOSP and lasted longer, too. And for the enhanced layer, March 10 is the same for all payloads and March 11 is found in EHSP and ELSP.

Payload		SOSP	SFSP	EHSP	ELSP
Recorded Energy		0.1-4MeV	40-300keV	0.2-20keV	10-1000eV
Increased Layer	Response energy	0.2-4MeV	40-300keV	0.5-20keV	unclear
	Starting Time	March 8	March 7	March 7	unclear
	Ending Time	March 12-13	March 12-16	March 12-14	unclear
Core Layer	Response energy	0.1 ~1MeV.	40-100keV	0.5-1keV	10-200eV
	Starting Time	March 10	March 10	March 10 & 11	March 10 & 11
	Ending Time	March 11	March 11	March 10 & 12	March 10 & 11

Table 1. Particle Flux change onboard WIND.

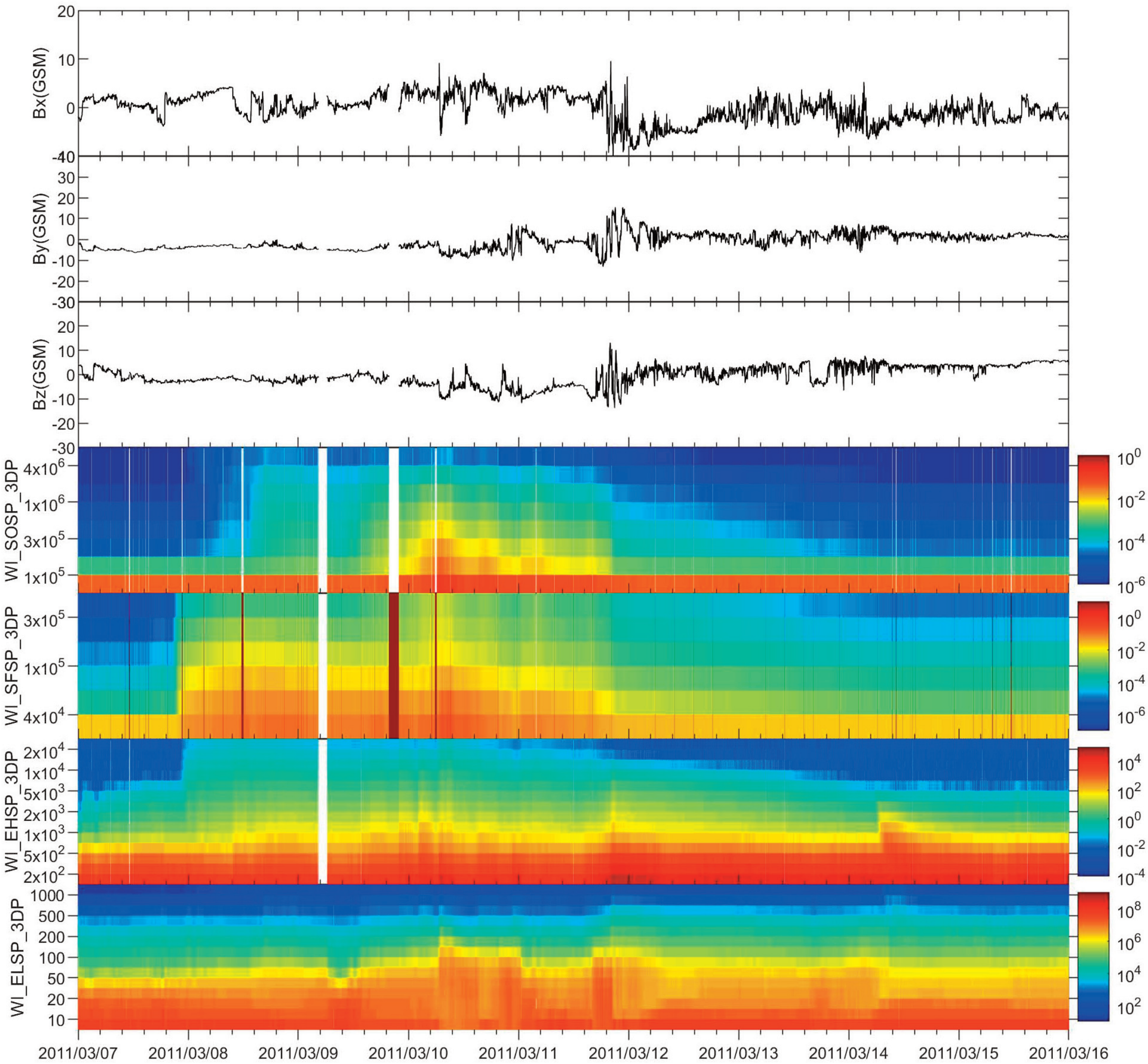

Figure 2. Magnetism and particle flux from WIND satellite.

2.4 CLUSTER II observatory

CLUSTER II is composed of four identical spacecraft flying in a tetrahedral formation, with an aim to study the impact of the Sun's activity on the Earth's space environment. Each orbit took approximately 57 hours to complete. Figure 3 shows the RAPID (Research with Adaptive Particle Imaging Detectors) particle flux from March 1 to March 16, 2011.

Figure 3 shows that normally the flux keeps steady and only increase quickly when they pass the perigee which is close to the polar region. The flux increases from March 8 to March 10 and then decreases to normal level.

2.5 GOES

The Geostationary Operational Environmental Satellites (GOES) all carry on the Space Environment Monitor (SEM) instrument at geosynchronous orbit around 6.6Re. The GOES Energetic Particle Sensor (EPS) measure proton, alpha-particle, and electron fluxes. GOES 13 was launched in 2006, located at 85.16° E and 0.36° S GOES 15 was launched in 2011 and located at 128.35° W and 0.03° S.

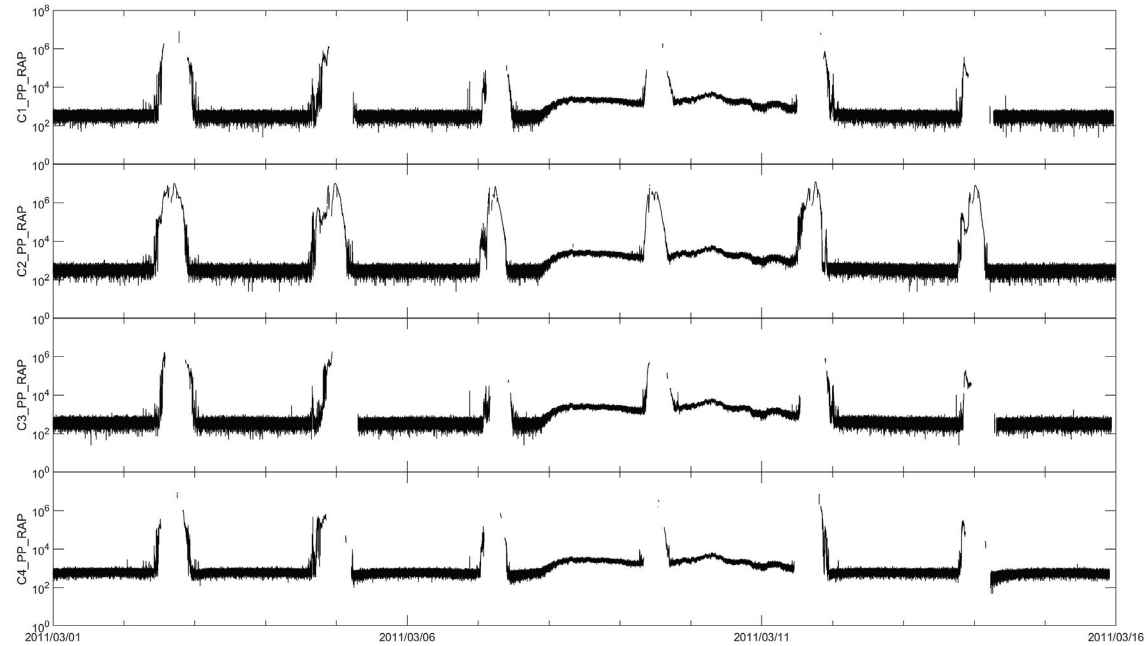

Figure 3. Cluster particle flux from March 1 to March 16, 2011; C1, C2,C3, C4 means the 4 satellites.

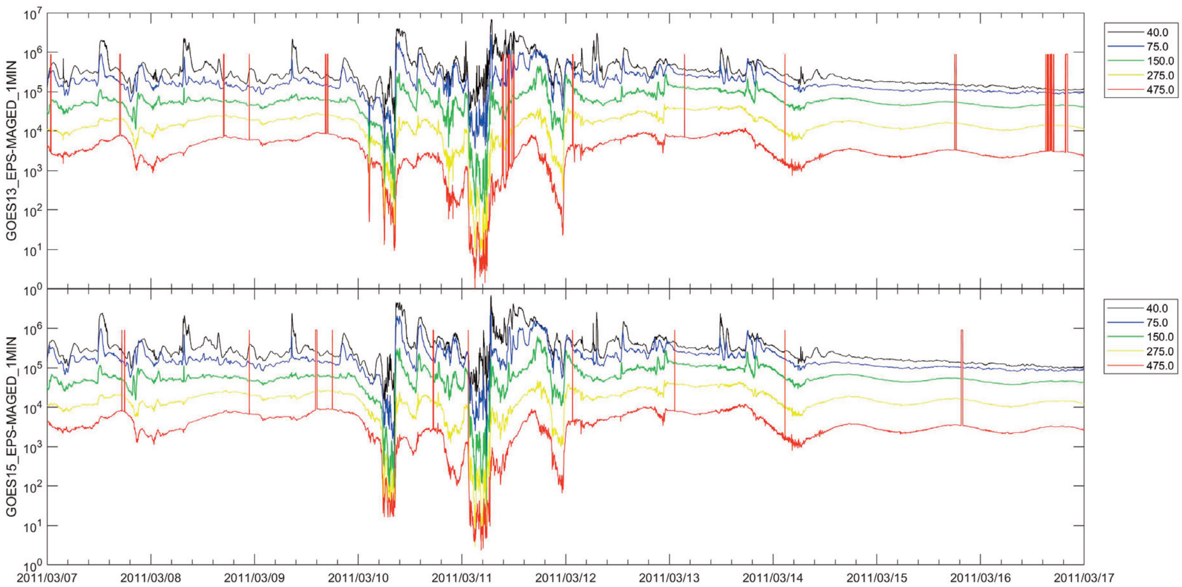

Figure 4. Particle flux from GOES 13 and 15.

The electron fluxes from GOES 13 and GOES 15 approximately present the same character (Figure 4). In the lower energy, such as 40eV, 75eV, the periodic daily pump can be found, but in higher energy, it is not so obvious. As shown in Figure 4, only three decreasingly rapid fluctuations on March 10 and March 11 are found from March 7 to March 17. The first two are before the earthquake and the third one is after the earthquake. For the middle one, the change amplitude is biggest. For the after one, the amplitude is smallest.

3. Analysis and Discussions

From Figure 1 to 4, each parameter has its variation and it is inconvenient to judge whether the variation is connected with the huge earthquake or not. Figure 5 gives some parameters with key time information. From T1 Line, it is clear that the increase in WIND from March 8 should be connected with the F10.7 high values. T2 line gives the beginning time of the main phase for this geomagnetic storm, and also explains the beginning time of enhancement in WIND and decrease in GOES. T3 and T4 give a period to show the 1st disturbance in GOES, the core enhancement in WIND and the 1st high value (> 40) in Kp. Then, T5 and T6 are for the 2nd one, and T8 and T9 are for the 3rd. T7 line gives the earthquake time which is about 14minutes later than T6. T6 is also the the lowest Dst time point for the geomagnetic storm.

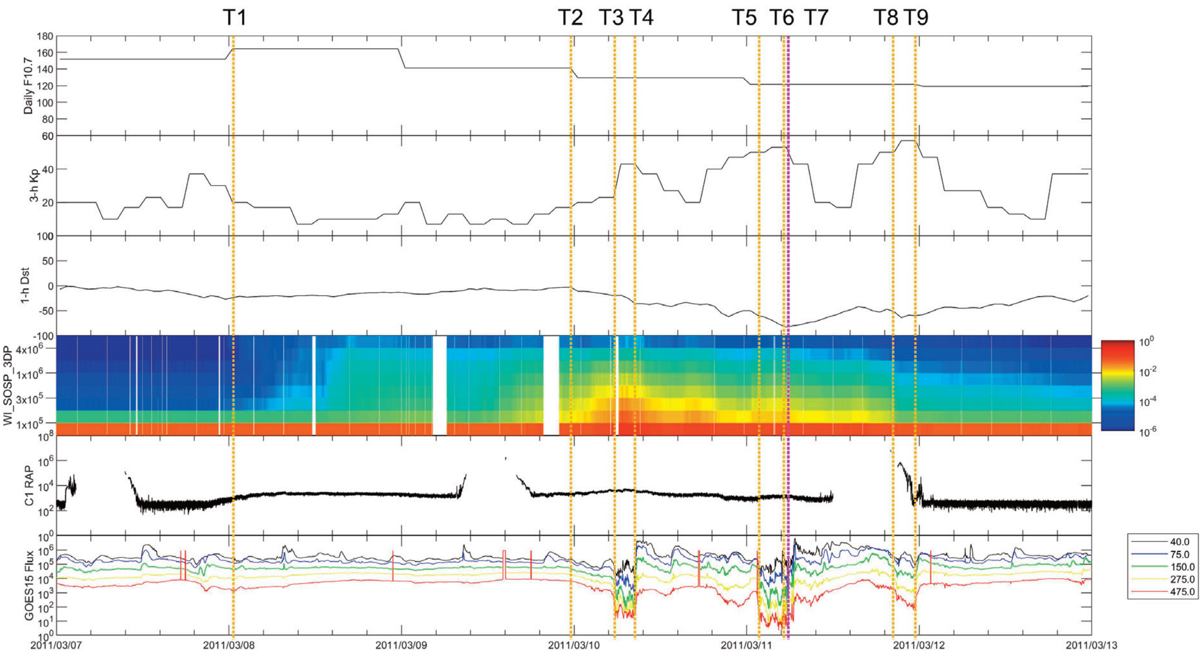

Figure 5. The jointly compassion of different parameters T1: the beginning time of F10.7 peak; T2: magnetic storm beginning time from Dst; T3: beginning time of the 1st GEOS flux disturbance; T4: ending time of the 1st GEOS flux disturbance; T5: beginning time of the 2nd GEOS flux disturbance; T6: ending time of the 2nd GEOS flux disturbance; T7: huge earthquake time; T8: beginning time of the 3rd GEOS flux disturbance; T9: ending time of the 3rd GEOS flux disturbance.

Considering the F10.7 and particle flux in WIND, they go in synchronization trend. For GOES, the situation is a little complex. For the 1st flux drop on March 10, the Kp is 4.3, and the corresponding change in particle flux is from ~6000 to ~20. For the second flux drop on March 11, the kp is 5.3, and the particle flux is from ~1000 to ~2. For the third one, the kp is 5.7 and the flux change is from ~6000 to ~100. In summary, the relative change ratio is 300, 500 and 60 but the spatial Kp is 4.3, 5.3 and 5.7. And based on previous research [He, et al, 2011], the changing amplitude is consistent with the geomagnetic storm intensity. So generally the change amplitudes of the previous two flux should be smaller than the third one. According to GPS TEC and infrasonic record, the coseismic ionospheric effect was recorded one hour after the earthquake (Hao, et al, 2012), then there is no after-seismic effect on the 3rd flux drops in GOES because particle flux drop is 19 hours later after the earthquake. So the third drop is only the effect of high Kp. Then there should be some other source which leads to the bigger drop during the T3-T4 and T5-T6. According to the analysis above, the only source may come from the pre-seismic electromagnetic emission of the coming huge earthquake on March 11. What's more, the duration of the lower flux values could also sustain the conclusion. For the third Kp, it is just a pulse. For the first, the duration is almost 3 hours, and for the second, the duration is almost 4.5 hours. During those durations, some local HF changes could be found which is far different from the spatial index frequency. So the possible pre-seismic effect should be considered for such two decreasing.

In addition, for the T3-T4 and T8-T9, there is no more variation after the kp decreases. While after T5-T6 and T7, the fluxes in GOES occur, which should be the coseismic effect to the energetic particles.

4. Conclusions

Using the various altitudes observations on WIND, CLUSTER and GOES, the high energetic particle fluxes are compared around the Tohoku huge earthquakes. The results indicate that:

All satellite with particle detectors could record the solar activity. And in low orbit satellite, GOES, could also record the pre- and co-seismic particle precipitation.

Particles with the different energy could response to the same source and the responding time and amplitude are different.

Although the spatial background is not quite, the pre-seismic information could be detected. And with more cases, the real pre-seismic energetic particle flux changes could be quantified.

Acknowledgement. Thanks to R. Lin/S. Bale at UC Berkeley, A. Szabo at NASA/GSFC for WIND and CLUSTER data and SWPC for the GOES data. Thanks SPDF, Goddard Space Flight Center, NASA for the CDAwebdata and figure support (http://cdaweb.gsfc.nasa.gov/istp_public/). Thanks for the f10.7 figure from Space Environment Prediction Center, National Space Science Center (http://www.sepc.ac.cn/F107Index_chn.php). This work is supported by the National State key R&D project (2018YFC1503501), ISSI-BJ(2019) and APSCO Earthquake Phase II. The authors would also like to thank reviewers and Editor for their valuable suggestions that have greatly improved this paper.

References

Aleksandrin, S.Yu., A.M. Galper, L.A. Grishantzeva, S.V. Koldashov, L.V. Maslennikov, A.M. Murashov, P. Picozza, V. Sgrigna, S.A. Voronov (2003), High energy charged particle bursts in the near-Earth space as earthquake precursors. Annales Geophysicae, 21, 597–602.doi:10.5194/angeo-21-597-2003

Fidani C., Battiston R. and W.J. Burger (2010). A Study of the Correlation between Earthquakes and NOAA Satellite Energetic Particle Bursts, Remote Sensing, 2, 2170-2184. DOI:10.3390/rs2092170

Galvan, D.A., A.Komjathy, M.P.Hickey, P.Stephens, J.Snively, Y.TonySong, M.D.Butala and A.J.Mannuci (2012). Ionospheric signatures of Tohoku-Oki tsunami of March 11, 2011: Model comparisons near the epicenter, Radio Sci., 47, RS4003, doi:10.1029/2012RS005023.

Galper, A.M., V.B. Dimitrenko, N.V. Nikitina, V.M. Grachev, S.E. Ulin (1989). Interrelation between high-energy charged particle fluxes in the radiation belt and seismicity of the Earth. Cosmic Research, 27, 789.

Galperin, Yu.I., V.A. Gladyshev, N.V. Jordjio, V.I. Larkina (1992). Precipitation of high-energy captured particles in the magnetosphere above the epicenter of an incipient earthquake. Cosmic Research, 30, 89–106.

Galper, A.M., S.V. Koldashov, S.A. Voronov (1995). High energy particle flux variations as earthquake predictors. Adv. Space Res., 15, 131–134. DOI:10.1016/0273-1177(95)00085-S

Hao, Y. Q., Z. Xia, and D. H. Zhang (2012). Multi-instrument observation on co-seismic ionospheric effects after great Tohoku earthquake, J. Geophys. Res., 117, A02305, doi:10.1029/2011JA017036.

He, Z.G., F. Xiao, Q. Zong, Y. Wang, L. Chen, C. Le, S. Zhang (2011). Multi-satellite observations on the storm-time enhancements of energetic outer zone electron fluxes driven by chorus waves. Sci. China Tech. Sci., 54: 2209-226, doi:10.1007/s11431-011-4445-6.

Heki, K. (2011), Ionospheric electron enhancement preceding the 2011Tohoku-Oki earthquake, Geophys. Res. Lett., 38, L17312, doi:10.1029/2011GL047908.

Heki, K. and Y. Enomoto (2013). Preseismic ionospheric electron enhancements revisited, J. Geophys. Res. Space Physics, 118, 6618–6626, doi:10.1002/jgra.50578.

Huang J.P., J. Liu, X.Y. Ouyang, W.J. Li. (2010). Analysis to the enegetic particles around the Chili Earthquake M 8.8. Seismology and Geology, 32(3): 417-423 (in Chinese with English abstract) DOI:10.3969/j.issn.0253-4967.2010.03.008.

Komjathy,A., D.A. Galvan, P. Stephens, M.Butala, V. Akopian, B.Wilson, O.Verkhoglyadova, A. Mannucci, M.P. Hickey (2012). Detecting Ionospheric TEC perturbations caused by natural hazards using a global network of GPS receivers: The Tohoku case study, Earth Planets Space, 64,1–8. DOI:10.5047/eps.2012.08.003.

Jin, S., R. Jin and J. H. Li (2014). Pattern and evolution of seismo-ionospheric disturbances following the 2011 Tohoku earthquakes from GPS observations, J. Geophys. Res. Space Physics, 119, 7914–7927, doi:10.1002/2014JA019825.

Kuo, C. L., L. C. Lee and J. D. Huba. (2014). An improved coupling model for the lithosphere-atmosphere-ionosphere system, J. Geophys. Res. Space Physics, 119, 3189–3205, doi:10.1002/2013JA019392.

Li, X., Y. Ma, P. Wang, H. Wang, H. Lu, X. Zhang, J. Huang, F. Shi, X. Yu, Y. Xu, X. Meng, H. Wang, X. Zhao, M. Parrot (2012). Study of the North West Cape electron belts observed by DEMETER satellite, J. Geophys. Res., 117, A04201, doi:10.1029/2011JA017121.

Merzer, M., S.L. Klemperer (1997). Modeling low-frequency magnetic-field precursors to the Loma Prieta earthquake with a precursory increase in fault-zone conductivity. Pure and Applied Geophys., 150, 217–248. DOI:10.1007/s000240050074

Molchanov, O.A., M. Hayakawa (1998). On the generation mechanism of ULF seismogenic electromagnetic emissions. Phys. Earth Planet. Int. 105, 201–210. DOI:10.1016/S0031-9201(97)00091-5

Nemec, F., O. Santolik and M. Parrot (2009). Decrease of intensity of ELF/VLF waves observed in the upper ionosphere close to earthquakes: A statistical study, J. Geophys. Res., 114, A04303, doi:10.1029/2008JA013972.

Parrot M. (2012). Statistical analysis of automatically detected ion density variations recorded by DEMETER and their relation to seismic activity, Ann. Geophys., 55(1): 149-155, doi:10.4401/5270.

Pulinets, S.A., K.A. Boyarchuk, V.V. Hegai, V.P. Kim, A. M. Lomonosov (2000). Quasielectrostatic model of atmosphere–thermosphere–ionosphere coupling. Adv. Space Res., 26, 1209–1218. DOI:10.1016/S0273-1177(99)01223-5

Pulinets, S. and K. Boyarchuk (2004). Ionospheric Precursors of Earthquakes, 315, Springer, Berlin, Germany.

Pulinets, S. and D. Ouzounov (2011). Lithosphere–Atmosphere–Ionosphere Coupling (LAIC) model – An unified concept for earthquake precursors validation, J. Southeast Asian Earth Sci., 41(4–5), 371–382, doi:10.1016/j.jseaes.2010.03.005.

Rozhnoi, M. Solovieva, O. Molchanov, P.-F. Biagi, M. Hayakawa, K. Schwingenschuh, M. Boudjada, and M. Parrot (2008). Variations of VLF/LF signals observed on the ground and satellite during a seismic activity in Japan region in May–June 2008, Nat. Hazards Earth Syst. Sci., 10, 529–534. doi:10.5194/nhess-10-529-2010

Russell, C. T., Janet G. Luhmann, Robert J. Strangeway. (2016). Space Physics. Cambridge University Press.

Sgrigna, V., L. Carota, L. Conti, M. Corsi, A. M. Galper, S. V. Koldashov, A. M. Murashov, P. Picozza, R. Scrimaglio and L. Stagni (2005). Correlations between earthquakes and anomalous particle bursts from SAMPEX/PET satellite observations, J. Atmos. Sol.-Terr. Phys., 67, 1448–1462. doi:10.1016/j.jastp.2005.07.008.

Pustovetov, V.P., A.B. Malyshev (1993). Space–time correlation of earthquakes and high-energy particle flux variations in the inner radiation belt, Cosmic Research, 31, 84–90.

Voronov, S.A., A.M Galper, S.V. Koldashov, L.V. Maslennikov, V.V. Mikhailov, N.V. Nikitina, A.V. Popov (1990). Increases in high energy charged particle fluxes near the South Atlantic Magnetic Anomaly and the seismicity of the Earth, Cosmic Research, 28, 789–791.

Walt, M., (1994). Introduction to Geomagnetically Trapped Radiation. Cambridge University Press, Cambridge.

Wang, P., Z. Chang, H. Wang and H. Lu (2014). Statistical similarity between high energy charged particle fluxes in near-earth space and earthquakes, Nat. Hazards Earth Syst. Sci. Discuss., 2, 3183-3192, https://doi.org/10.5194/nhessd-2-3183-2014.

Yu, Y., Z. Yan and M. P. Hickey (2015). Lower thermospheric response to atmospheric gravity waves induced by the 2011 Tohoku tsunami, J. Geophys.Res. Space Physics, 120, 5062–5075,doi:10.1002/2015JA020986.

Zhang X., X. Shen, S. Zhao, Lu Yao, X. Ouyang, J. Qian (2014). The characteristics of quasistatic electric field perturbations observed by DEMETER satellite before large earthquakes, J. Asian Earth Sci., 79, 42–52. doi:10.1016/j.jseaes.2013.08.026.

Zhang X., X. Shen, M. Parrot, Z. Zeren, X. Ouyang., J. Liu, J. Qian, S. Zhao and Y. Miao (2012). Phenomena of electrostatic perturbations before strong earthquakes (2005-2010) observed on DEMETER, Nat. Hazards Earth Syst. Sci., 12, 75-83. doi:10.5194/nhess-12-75-2012.

Zhang X.,C. Fidani, J. Huang, X. Shen, Z. Zeren and J. Qian (2013). Burst increases of precipitating electrons recorded by the DEMETER satellite before strong earthquakes, Nat. Hazards Earth Syst. Sci., 13, 197-209, doi:10.5194/nhess-13-197-2013

Zhao S F, X. Shen, W. Pan, X. Zhang, L. Liao (2010). Penetration characteristics of VLF wave from atmosphere into lower ionosphere, Earthquake Science, 23, 275-282, doi:10.1007/s11589-010-0723-9

***CORRESPONDING AUTHOR: Jianping HUANG,**
National Institute of Natural Hazards,
Ministry of Emergency Management,
Beijing 100085, China
and Institute of Disaster Prevention,
Sanhe 065201, China,
e-mail: xhhjp@126.com